

# Unified description of turbulent entrainment

Maarten van Reeuwijk<sup>1</sup>, J. Christos Vassilicos<sup>2</sup> and John Craske<sup>1</sup>

<sup>1</sup>Department of Civil and Environmental Engineering,  
Imperial College London, London SW7 2AZ, UK

<sup>2</sup>Univ. Lille, CNRS, ONERA, Arts et Metiers ParisTech, Centrale Lille, FRE 2017 - LMFL -  
Laboratoire de Mécanique des fluides de Lille - Kampé de Fériet, F-59000 Lille, France

(Received xx; revised xx; accepted xx)

Integral equations are derived that describe turbulent free shear flows developing in space and/or time. The description clarifies the connection between the local (small-scale) and global (integral) descriptions of turbulent entrainment, and provides a seamless connection between the implicit description of the turbulent-nonturbulent interface (TNTI) required for the former and the explicit description of the TNTI usually adopted for the latter. The description is applied to the axisymmetric jet, the planar wake, temporal jet and unsteady jets and plumes.

## 1. Introduction

Despite over half a century of research and several review articles (e.g. Turner 1986; Fernando 1991; Woods 2010; de Rooy 2013; Da Silva *et al.* 2014; Mellado 2017), our understanding of turbulent entrainment (the transport of fluid from regions of relatively low to relatively high levels of turbulence) remains fragmented. One important reason is that turbulent entrainment is notoriously difficult to determine. Entrainment is a process that typically occurs over much larger timescales than turbulent timescales, and its effects are therefore easily obfuscated by turbulent fluctuations and transient effects. Furthermore, the quantification of turbulent entrainment requires the determination of a turbulent and non-turbulent (or less turbulent) region which is, by definition, arbitrary and thus subject to uncertainty.

However, there are other reasons that the understanding of turbulent entrainment remains challenging. One challenge is the sheer number of flows in which turbulent entrainment plays a role. Developing boundary layers can be classified based on the number of independent variables on which their solution depends, with a further distinction between statistically steady and unsteady problems, as shown in table 1. Consider a turbulent velocity field  $\mathbf{u}(x, y, z, t)$ , which will generally not have any symmetries. By ensemble averaging this velocity field, denoted by  $\bar{\cdot}$ , an average velocity field  $\bar{\mathbf{u}}$  is obtained which satisfies the symmetries present in the problem formulation (such as axisymmetric or streamwise homogeneity). In table 1,  $x$  is the (slowly developing) streamwise direction, and  $z$  or  $r$  is the normal direction, where  $z$  would be used for planar problems and  $r$  for axisymmetric problems. The class of steady problems with two independent variables comprises e.g. planar and axisymmetric jets (Hussein *et al.* 1994; Da Silva & Métais 2002; Westerweel *et al.* 2005; Watanabe *et al.* 2014), plumes (List 1982), wakes (Cantwell & Coles 1983; Obligado *et al.* 2016), fountains (Hunt & Burridge 2015), boundary layers (Head 1958; Sillero *et al.* 2013), mixing layers (Rajaratnam 1976) and inclined gravity currents (Wells *et al.* 2010; Odier *et al.* 2014; Krug *et al.* 2015).

In the class of unsteady problems with two independent variables are problems that develop slowly in time in one spatial dimension  $z$  or  $r$ . These are problems such as

TABLE 1. Classification of free shear flows based on the number of independent variables.

Dims	Steady	Unsteady
1	$\bar{\mathbf{u}}(z)$ (not encountered in free shear flows)	$\bar{\mathbf{u}}(t)$ (not encountered in free shear flows)
2	$\bar{\mathbf{u}}(x, z), \bar{\mathbf{u}}(x, r)$ jets, wakes, mixing layers, plumes, inclined gravity currents, ...	$\bar{\mathbf{u}}(z, t), \bar{\mathbf{u}}(r, t)$ Temporal jets, wakes, mixing layers, plumes, inclined gravity currents, penetrative convection, convective boundary layer, ...
3	$\bar{\mathbf{u}}(x, y, z)$ 2D gravity currents, stratified wakes, jets and plumes in crossflow, ...	$\bar{\mathbf{u}}(x, z, t), \bar{\mathbf{u}}(x, r, t)$ Unsteady versions of those in the category of 2D steady flows, e.g. unsteady jets, plumes, ...

penetrative convection (Mellado 2012; Holzner & van Reeuwijk 2017), convective and stable boundary layers (as relevant to the atmospheric boundary layer and the oceanic mixed layer; Kato & Phillips 1969; Deardorff 1980; Sullivan *et al.* 1998; Jonker *et al.* 2013; Garcia & Mellado 2014), stratocumulus clouds (Mellado 2017), but also include temporal jets (Da Silva & Pereira 2008; van Reeuwijk & Holzner 2014), plumes (Krug *et al.* 2017), gravity currents (van Reeuwijk *et al.* 2018, 2019), wakes (Redford *et al.* 2012; Watanabe 2016), mixing layers (Watanabe *et al.* 2018) and compressible reacting mixing layers (Jahanbakhshi & Madnia 2018). These temporal flows are not generally encountered in nature but share many of the features of their 2D steady cousins. However, with two homogeneous spatial directions, they are ideal for exploration with direct numerical simulation.

Steady problems with three independent variables possess two normal directions in which the flow develops ‘fast’ but in an anisotropic manner. Examples are jets and plumes discharged vertically in a crosswind (Mahesh 2013; De Wit *et al.* 2014; Woods 2010; Devenish *et al.* 2010), stratified wakes (Xu *et al.* 1995) and horizontally discharged point releases in stratified layers. The class of unsteady problems with three independent variables comprises all the flows mentioned in the category of 2D steady developing boundary layers, provided that one of their boundary conditions or the environment changes in time. Examples include unsteady jets and plumes (Scase *et al.* 2006; Craske & van Reeuwijk 2015, 2016; Woodhouse *et al.* 2016) and starting plumes (Turner 1962).

The examples mentioned in table 1 are encountered in different scientific fields ranging from engineering to oceanography to the meteorological sciences, and often employ slightly different ways to define entrainment (Hunt *et al.* 1983; de Rooy 2013; van Reeuwijk & Holzner 2014). Furthermore, there is always freedom in the choice of the characteristic scales of a problem to within a constant of proportionality, which can have a strong effect on the value of the entrainment coefficient  $V_n/\hat{u}$ , where  $V_n$  is the entrainment velocity and  $\hat{u}$  is a characteristic velocity. A classical example is the difference in the entrainment coefficient of turbulent jets and plumes based on top-hat and Gaussian profiles (see e.g. van Reeuwijk & Craske 2015), which differ by a factor  $\sqrt{2}$ .

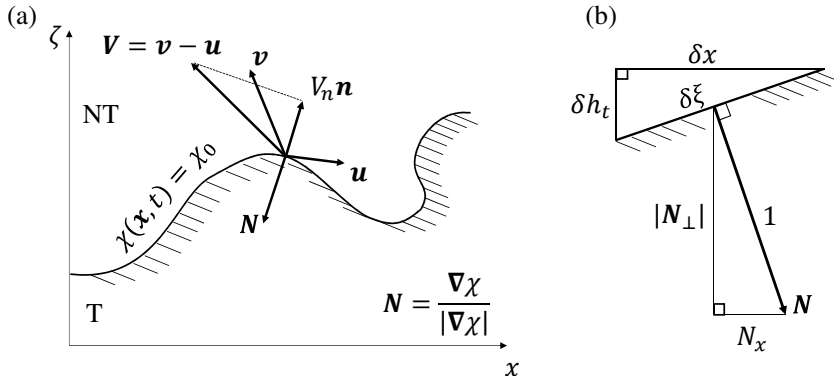


FIGURE 1. Interface properties of the turbulent-nonturbulent interface (TNTI) separating turbulent (T) from non-turbulent (NT) fluid. (a) Definition sketch. (b) Geometric properties.

Turbulent entrainment is generally studied either from a local or a global perspective. The global approach involves inferring the entrainment velocity from the Reynolds-averaged equations (e.g. Turner 1986) and considers entrainment from an integral perspective. The local approach, as pioneered by Corrsin & Kistler (1955), considers the microscale perspective. The local approach starts from choosing a scalar quantity  $\chi$  to provide an implicit definition of the instantaneous turbulent-nonturbulent interface (TNTI), where a threshold value  $\chi_0$  is used to distinguish the turbulent zone ( $\chi \geq \chi_0$ ) from the nonturbulent zone ( $\chi < \chi_0$ ). The most commonly used scalar quantity is enstrophy (e.g. Bisset *et al.* 2002; Holzner & Luethi 2011; Da Silva *et al.* 2014; van Reeuwijk & Holzner 2014), which is consistent with Corrsin & Kistler (1955), but passive scalars (e.g. Sreenivasan *et al.* 1989; Westerweel *et al.* 2005; BurrIDGE *et al.* 2017) or the turbulence kinetic energy (Philip *et al.* 2014) are also used to define the TNTI.

The velocity  $\mathbf{v}$  associated with any trajectory on an isosurface of  $\chi$  satisfies

$$\frac{d\chi}{dt} = \frac{\partial\chi}{\partial t} + \mathbf{v} \cdot \nabla\chi = 0. \quad (1.1)$$

By introducing a relative velocity  $\mathbf{V} = \mathbf{v} - \mathbf{u}$ , which is the difference between the isosurface velocity  $\mathbf{v}$  and the fluid velocity  $\mathbf{u}$ , (1.1) can be rewritten as (Holzner & Luethi 2011)

$$V_n = -\frac{1}{|\nabla\chi|} \frac{D\chi}{Dt}, \quad (1.2)$$

where  $D/Dt = \partial/\partial t + \mathbf{u} \cdot \nabla$  is the material derivative,  $V_n = \mathbf{V} \cdot \mathbf{N}$  is the normal component of the relative velocity and  $\mathbf{N} = \nabla\chi/|\nabla\chi|$  is the (3D) normal vector pointing into the turbulent region (Figure 1(a)). Note that the other two components of  $\mathbf{V}$  tangential to the isosurface are not specified by this definition. For an entraining flow,  $V_n < 0$ , which is a consequence of defining a normal  $\mathbf{N}$  that points *into*  $\Omega$ . The inward pointing normals also has consequences for the Gauss divergence theorem. By substituting the governing equation for  $\chi$  (usually enstrophy) into (1.2) and averaging, local aspects of turbulent entrainment can be explored (e.g. Holzner & Luethi 2011; Da Silva *et al.* 2014; van Reeuwijk & Holzner 2014; Krug *et al.* 2015; Jahanbakhshi & Madnia 2018).

The aim of this paper is to derive an integral description of free shear flows capable of representing both the local and global viewpoints of turbulent entrainment. Importantly, it will provide a unified description of entrainment in temporal problems (2D unsteady; Da Silva & Pereira 2008; van Reeuwijk & Holzner 2014; Krug *et al.* 2017), in which the TNTI moves but there is no net flow into the turbulent layer ( $V_n$  produced by  $\mathbf{v}$ ), spatial

problems (2D steady; Rajaratnam 1976; Turner 1986; Philip *et al.* 2014), in which the TNTI is statistically steady but there is a net flow into the turbulent layer ( $V_n$  produced by  $\mathbf{u}$ ), and unsteady free shear layers (3D unsteady; Craske & van Reeuwijk 2016).

## 2. The instantaneous integral continuity and momentum equations

In this section we present *instantaneous* integral volume (i.e. continuity) and momentum conservation equations. The focus of this work is on turbulent free shear flows which develop slowly (in a statistical sense) in time  $t$ , in the spatial direction  $x$ , or both. The incompressible Navier-Stokes equations are given by

$$\nabla \cdot \mathbf{u} = 0, \quad (2.1)$$

$$\frac{D\mathbf{u}}{Dt} = -\frac{1}{\rho_0} \nabla p + \nabla \cdot \boldsymbol{\tau} + \mathbf{f}, \quad (2.2)$$

where  $\boldsymbol{\tau}$  denotes the viscous stress tensor and  $\mathbf{f}$  is a body force. These equations will be integrated over the turbulent region in the  $y-z$  plane which is denoted  $\Omega$ . The following identities for the integrals of the gradient, divergence and material derivative operators can be derived:

$$\int_{\Omega} \nabla \phi dA = \frac{\partial}{\partial x} \int_{\Omega} \phi dA \mathbf{e}_x - \oint_{\partial\Omega} \phi \frac{\mathbf{N}}{|\mathbf{N}_{\perp}|} dl, \quad (2.3)$$

$$\int_{\Omega} \nabla \cdot \mathbf{F} dA = \frac{\partial}{\partial x} \int_{\Omega} F_x dA - \oint_{\partial\Omega} \mathbf{F} \cdot \frac{\mathbf{N}}{|\mathbf{N}_{\perp}|} dl, \quad (2.4)$$

$$\int_{\Omega} \frac{D\phi}{Dt} dA = \frac{\partial}{\partial t} \int_{\Omega} \phi dA + \frac{\partial}{\partial x} \int_{\Omega} u_x \phi dA - \int_{\Omega} \phi \nabla \cdot \mathbf{u} dA + \oint_{\partial\Omega} \frac{V_n}{|\mathbf{N}_{\perp}|} \phi dl, \quad (2.5)$$

where  $\phi$  is an arbitrary scalar or vector component field and  $\mathbf{F}$  is an arbitrary vector field. Vectors with a perp ( $\perp$ ) subscript denote the components perpendicular to the  $x$ -direction, i.e.  $\mathbf{F} = [F_x, \mathbf{F}_{\perp}]^T$ , and  $\nabla_{\perp} = [\partial/\partial y, \partial/\partial z]^T$ . The unit vector  $\mathbf{N} = \nabla\chi/|\nabla\chi|$  is normal to the 3D surface  $\chi = \chi_0$  which demarcates between turbulent and non-turbulent regions. The normal vector can be written as  $\mathbf{N} = [N_x, \mathbf{N}_{\perp}]^T$ , so that  $|\mathbf{N}_{\perp}|$  is the magnitude of the 3D normal in the  $y-z$  plane (see figure 1(b)). Finally,  $\mathbf{e}_x$  is the unit vector in the  $x$ -direction and  $u_x$  is the component of the fluid velocity field  $\mathbf{u}$  in that same direction. An easily accessible yet rigorous proof of these three identities is given in Appendix A. A more general derivation using differential geometry, which highlights the role of Stokes' theorem and the Leibniz integral rule, is given in Appendix B.

Noting that  $\nabla \cdot \mathbf{u} = D\phi/Dt$  for  $\phi = 1$  and using (2.5) implies that the instantaneous integral continuity equation is given by

$$\frac{\partial}{\partial t} \int_{\Omega} dA + \frac{\partial}{\partial x} \int_{\Omega} u_x dA = - \oint_{\partial\Omega} \frac{V_n}{|\mathbf{N}_{\perp}|} dl. \quad (2.6)$$

Note that if the relative isosurface velocity  $\mathbf{V}$  is everywhere tangential to the interface then  $V_n = 0$ , in which case (2.6) describes a streamtube. Entrainment allows exchange across the isosurface  $\chi = \chi_0$ . For an entraining flow,  $V_n < 0$  (due to the inward pointing normal).

The line integral represents the net entrainment into the turbulent region. The presence of  $|\mathbf{N}_{\perp}|$  is representative for the projection of the 3D quantity  $V_n$  onto the  $y-z$  plane. This is better seen by using  $V_n = \mathbf{V} \cdot \mathbf{N}$  to write the entrainment term as

$$\oint_{\partial\Omega} \frac{V_n}{|\mathbf{N}_{\perp}|} dl = \oint_{\partial\Omega} \mathbf{V}_{\perp} \cdot \mathbf{n} dl + \oint_{\partial\Omega} V_x \frac{N_x}{|\mathbf{N}_{\perp}|} dl, \quad (2.7)$$

where  $\mathbf{n} = \nabla_{\perp}\chi/|\nabla_{\perp}\chi|$  is the normal in the  $y - z$  plane, and note that this quantity is related to the 3D normal via  $\mathbf{n} = \mathbf{N}_{\perp}/|\mathbf{N}_{\perp}|$ . The first term on the right-hand side of (2.7) is simply the entrainment flux arising from the in-plane relative velocity components  $\mathbf{V}_{\perp}$ . As described in appendices A and B, the second term on the right-hand side of (2.7) arises from the commutation of integration and differentiation with respect to  $x$  that is required to formulate (2.6). It represents the net transport of the streamwise relative velocity component  $V_x$  into the turbulent region across the interface whose local slope is  $N_x/|\mathbf{N}_{\perp}|$  (see Figure 1).

Integration over the region  $\Omega$  of (2.2) and use of identities (2.3)-(2.5) results in

$$\begin{aligned} \frac{\partial}{\partial t} \int_{\Omega} \mathbf{u} \, dA + \frac{\partial}{\partial x} \int_{\Omega} \left( u_x \mathbf{u} + \frac{p}{\rho_0} \mathbf{e}_x \right) \, dA = \\ - \oint_{\partial\Omega} \frac{1}{|\mathbf{N}_{\perp}|} \left( V_n \mathbf{u} - \frac{p}{\rho_0} \mathbf{N} \right) \, d\ell + \int_{\Omega} \mathbf{f} \, dA. \end{aligned} \quad (2.8)$$

Here, the shear-stress contributions have been neglected as is conventional for high Reynolds free shear flows. Equations (2.6) and (2.8) are instantaneous.

### 3. Local averaged integral equations

In this section we present the averaged integral equations for volume and momentum conservation. These provide information about the local aspects of turbulent entrainment as they stem from ensemble averaging of the *instantaneous* integral equations. Performing ensemble averaging, denoted by the overbar  $\bar{\cdot}$ , on the instantaneous integrated continuity equation (2.6) and the streamwise  $x$ -component of the integrated momentum equation (2.8) yields

$$\frac{\partial}{\partial t} \overline{\int_{\Omega} dA} + \frac{\partial}{\partial x} \overline{\int_{\Omega} u_x \, dA} = - \overline{\oint_{\partial\Omega} \frac{V_n}{|\mathbf{N}_{\perp}|} \, d\ell}, \quad (3.1)$$

$$\begin{aligned} \frac{\partial}{\partial t} \overline{\int_{\Omega} u_x \, dA} + \frac{\partial}{\partial x} \overline{\int_{\Omega} \left( u_x^2 + \frac{p}{\rho_0} \right) \, dA} = \\ - \overline{\oint_{\partial\Omega} \frac{1}{|\mathbf{N}_{\perp}|} \left( V_n u_x - \frac{p}{\rho_0} N_x \right) \, d\ell} + \overline{\int_{\Omega} f_x \, dA}. \end{aligned} \quad (3.2)$$

In the integral continuity equation (3.1),  $\overline{\int_{\Omega} dA}$  represents the average instantaneous cross-sectional area of the turbulent region at location  $x$ . It is not possible to commute the integral with the ensemble averaging because the integration regions  $\Omega$  and  $\partial\Omega$  vary in time and per ensemble instance.

### 4. Global averaged integral equations

Equations (3.1), (3.2) ultimately link the integral behaviour of the free shear flow to the small-scale dynamics at the TNTI when  $\chi$  is an instantaneous quantity. The global, integral dynamics can be obtained by using an *average* quantity  $\bar{\chi}$  with associated threshold  $\bar{\chi}_0$  to identify the interface. By considering an average quantity, the TNTI will not be contorted but will be smooth and satisfy the symmetries corresponding to homogeneity in the problem under consideration.

## 4.1. Non-slender flows

Using  $\bar{\chi}$  to define the 3D normal results in  $\mathbf{N} = \nabla\bar{\chi}/|\nabla\bar{\chi}|$ , which implies that  $\overline{\mathbf{V} \cdot \mathbf{N}} = \overline{\mathbf{V}} \cdot \mathbf{N}$ . Using  $\mathbf{V} = \mathbf{v} - \mathbf{u}$  and expanding results in the exact expression

$$\bar{V}_n = (\bar{\mathbf{v}} - \bar{\mathbf{u}}) \cdot \mathbf{N} = \frac{\bar{\mathbf{v}} \cdot \nabla\bar{\chi} - \bar{\mathbf{u}} \cdot \nabla\bar{\chi}}{|\nabla\bar{\chi}|} = -\frac{1}{|\nabla\bar{\chi}|} \frac{D\bar{\chi}}{Dt}, \quad (4.1)$$

where  $\overline{D/Dt} = \partial/\partial t + \bar{\mathbf{u}} \cdot \nabla$  and use was made of (1.2) for  $\chi = \bar{\chi}$ .

An advantage of considering averaged quantities is that it is possible to represent the isosurface  $\bar{\chi} = \bar{\chi}_0$  (which implicitly defines the TNTI) *explicitly* in terms of a single-valued function  $h_t$ . Restricting attention to planar or axisymmetric problems, a scalar level-set function  $L(x, \zeta, t) = h_t(x, t) - \zeta$  can be constructed such that  $L = 0$  represents the average interface position where  $\zeta$  is the direction normal to the interface. Setting  $\bar{\chi} = L$  implies that (4.1) can be equivalently be expressed as

$$\bar{V}_n = -\frac{1}{|\nabla L|} \left( \frac{Dh_t}{Dt} - \frac{D\zeta}{Dt} \right) = \frac{1}{|\nabla L|} \left( \bar{u}_\zeta - \frac{Dh_t}{Dt} \right), \quad (4.2)$$

where  $|\nabla L| = \sqrt{1 + (\partial h_t / \partial x)^2}$ .

Because the interface is based on the average quantity  $\bar{\chi}$ , the averaging and integral operators *do* commute, which implies that (3.1), (3.2) simplify to

$$\frac{\partial}{\partial t} \int_{\bar{\Omega}} dA + \frac{\partial}{\partial x} \int_{\bar{\Omega}} \bar{u}_x dA = - \oint_{\partial\bar{\Omega}} \frac{\bar{V}_n}{|\mathbf{N}_\perp|} dl, \quad (4.3)$$

$$\begin{aligned} \frac{\partial}{\partial t} \int_{\bar{\Omega}} \bar{u}_x dA + \frac{\partial}{\partial x} \int_{\bar{\Omega}} \left( \bar{u}_x^2 + \frac{\bar{p}}{\rho_0} \right) dA = \\ - \oint_{\partial\bar{\Omega}} \frac{1}{|\mathbf{N}_\perp|} \left( \overline{V_n u_x} - \frac{\bar{p}}{\rho_0} N_x \right) dl + \int_{\bar{\Omega}} \bar{f}_x dA. \end{aligned} \quad (4.4)$$

Here, we have denoted the integration domain and boundary with  $\bar{\Omega}$  and  $\partial\bar{\Omega}$ , respectively, to distinguish from the local viewpoint. The integrals can be made definite once a specific coordinate system is selected. Note that  $\bar{u}_x^2 = \overline{u_x^2} + \overline{u_x' u_x'}$ .

## 4.2. Slender flows

Many free shear flows have the additional property of being *slender*, i.e. they develop much more slowly in the streamwise  $x$ -direction than in the normal direction, which implies that, apart from all quantities changing slowly in the  $x$ -direction,  $\partial\bar{\chi}/\partial x \ll |\nabla_\perp \bar{\chi}|$ . Under the assumption of slenderness, (4.1), (4.2) become

$$\bar{V}_n = -\frac{1}{|\nabla_\perp \bar{\chi}|} \frac{D\bar{\chi}}{Dt} = \bar{u}_\zeta - \frac{Dh_t}{Dt}. \quad (4.5)$$

The assumption of slenderness also implies that  $|N_x| \ll |\mathbf{N}_\perp|$ , which furthermore implies that  $|\mathbf{N}_\perp| \approx 1$  and  $\mathbf{N}_\perp \approx \mathbf{n}$ . Thus, under this assumption the equations (4.3,4.4) further simplify to

$$\frac{\partial}{\partial t} \int_{\bar{\Omega}} dA + \frac{\partial}{\partial x} \int_{\bar{\Omega}} \bar{u}_x dA = - \oint_{\partial\bar{\Omega}} \bar{V}_n dl, \quad (4.6)$$

$$\begin{aligned} \frac{\partial}{\partial t} \int_{\bar{\Omega}} \bar{u}_x dA + \frac{\partial}{\partial x} \int_{\bar{\Omega}} \left( \bar{u}_x^2 + \frac{\bar{p}}{\rho_0} \right) dA \\ = - \oint_{\partial\bar{\Omega}} \left( \overline{V_n u_x} - \frac{\bar{p}}{\rho_0} N_x \right) dl + \int_{\bar{\Omega}} \bar{f}_x dA. \end{aligned} \quad (4.7)$$

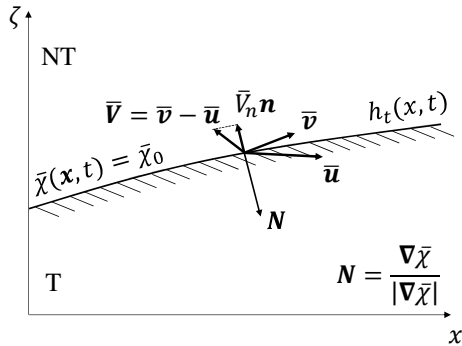


FIGURE 2. Definition sketch of the global (average) perspective on the turbulent-nonturbulent interface (TNTI).

#### 4.3. Linking $h_t$ to characteristic quantities

Integral models that rely on a global entrainment velocity do not typically make explicit reference to a scalar interface  $h_t$ . Instead, a characteristic width of the flow  $h$  is defined from either

(i) the specific features of a given velocity profile, such as the centreline velocity  $\bar{u}_x(x, 0)$  and the half-width  $h_{1/2}$ , such that  $\bar{u}_x(x, h_{1/2}) = \bar{u}_x(x, 0)/2$ . Such definitions are commonly used in conjunction with self-similarity (Rajaratnam 1976; Pope 2000) and Gaussian velocity profiles (Kotsovinos & List 1977).

(ii) integral quantities that make no reference to the underlying velocity profiles. For the example of an axisymmetric jet, one would calculate the volume flux  $Q = 2 \int \bar{u}_x r dr$  and specific momentum flux  $M = 2 \int \bar{u}_x^2 r dr$  (per unit radian) and define a characteristic (so-called ‘top-hat’) width  $h = Q/\sqrt{M}$ .

For self-similar flows, the approaches (i) and (ii) determine the prefactor or proportionality coefficient involved in the corresponding definition of entrainment and therefore play an influential, albeit superficial, role in studies of entrainment. In contrast, the volume flux  $Q$  in (ii) is useful in relating directly to a quantity that has a clear physical meaning and relationship with (4.6), but must make use of a threshold to define the upper limit of the integral of  $\bar{u}_x$  (such as  $\chi = \bar{u}_x(x, r)/\bar{u}_x(x, 0) = 0.01$ ). Indeed, the formal integrals of  $\bar{u}_x(x, r)$  to  $r \rightarrow \infty$  that are widely used in plume theory are, depending on the boundary conditions imposed on the induced irrotational flow, not necessarily well-defined (Kotsovinos 1978). A further complication arises in flows that are not self-similar, which makes it impossible to relate  $h$  with  $h_t$  using a constant of proportionality (see §6.4). These issues will be discussed in greater detail in §6.

## 5. Connecting the local and global viewpoints

The integral representations of the local and global continuity equations, (3.1) and (4.3) respectively, can be used to establish the relation between the local entrainment velocity  $V_n$  and the global entrainment velocity  $\bar{V}_n$ . Indeed, assuming that the thresholds  $\chi_0$  and  $\bar{\chi}_0$  are taken sufficiently small such that the entire turbulent region is captured, the left-hand sides of (3.1) and (4.3) are approximately equal. This implies that

$$\oint_{\partial\Omega} \frac{V_n}{|\mathbf{N}_\perp|} d\ell = \oint_{\partial\bar{\Omega}} \frac{\bar{V}_n}{|\bar{\mathbf{N}}_\perp|} d\ell. \quad (5.1)$$

Consistent with Zhou & Vassilicos (2017), we introduce the average instantaneous interface and average interface lengths as  $\mathcal{L} = \overline{\oint_{\partial\Omega} d\ell}$  and  $\bar{\mathcal{L}} = \oint_{\partial\bar{\Omega}} d\ell$ , respectively. Note that  $\bar{\mathcal{L}}$  can be determined straightforwardly from the problem geometry and  $h_t$  (see also §6). The average instantaneous interface length  $\mathcal{L}$  is expected to scale in a fractal manner (Sreenivasan *et al.* 1989), implying that  $\mathcal{L} \gg \bar{\mathcal{L}}$  for  $Re \gg 1$ . Equation (5.1) can be recast as (van Reeuwijk & Holzner 2014; Zhou & Vassilicos 2017)

$$\frac{\langle \bar{V}_n \rangle}{\langle V_n \rangle} = \frac{\mathcal{L}}{\bar{\mathcal{L}}}, \quad (5.2)$$

where  $\langle V_n \rangle = \mathcal{L}^{-1} \overline{\oint_{\partial\Omega} V_n / |\mathbf{N}_\perp| d\ell}$  and  $\langle \bar{V}_n \rangle = \bar{\mathcal{L}}^{-1} \oint_{\partial\bar{\Omega}} \bar{V}_n / |\mathbf{N}_\perp| d\ell$  are the effective local and global entrainment velocity, respectively. The fractal arguments for  $\mathcal{L}$  can imply that the local entrainment velocity  $\langle V_n \rangle$  is of the order of the Kolmogorov velocity (Corrsin & Kistler 1955; van Reeuwijk & Holzner 2014; Silva *et al.* 2018) for a specific value of the fractal dimension of the interface, but Zhou & Vassilicos (2017) also argued for the possibility of a different scaling, independent of the value of the fractal dimension, in the presence of non-equilibrium turbulence. It must be noted, however, that the definition of local entrainment velocity used by Zhou & Vassilicos (2017) actually relates to a pseudo-velocity (see Appendix A and section B.2 of Appendix B). Even so, their local entrainment velocity does scale with the Kolmogorov velocity in the presence of classical equilibrium turbulence.

## 6. Special cases

In this section we will apply the integral description to four canonical free shear flows, namely the axisymmetric jet, the planar wake, the temporal jet and unsteady axisymmetric jets/plumes. As turbulent free shear flows are characterised by a high Reynolds number  $Re$  and a slow development in the  $x$  (or  $t$ ) direction, the governing equations are the boundary layer equations which neglect viscous stresses and pressure. It will be assumed that the streamwise velocity  $\bar{u}_x$  is used to define the turbulent region for the global entrainment, i.e.  $\bar{\chi} = \bar{u}_x$ . Furthermore, consistent with general practice on thresholding, all quantities of  $O(\bar{\chi}_0)$  will be assumed negligible.

### 6.1. Axisymmetric jet

The axisymmetric jet is homogeneous in the azimuthal direction  $\theta$  and time  $t$ . Applying the symmetries to (4.5) and setting  $\zeta = r$ , we have

$$\bar{V}_n = \bar{u}_r(x, h_t). \quad (6.1)$$

Thus, (4.6), (4.7) are given by, using that  $dA = 2\pi r dr$  and  $\bar{\mathcal{L}} = 2\pi h_t$ :

$$2\pi \frac{d}{dx} \int_0^{h_t} \bar{u}_x r dr = -2\pi h_t \bar{V}_n = -2\pi h_t \bar{u}_r, \quad (6.2)$$

$$2\pi \frac{d}{dx} \int_0^{h_t} \frac{\bar{u}_x^2}{x} r dr = 0, \quad (6.3)$$

which is consistent with straightforward integration of the Reynolds-averaged boundary layer equations (e.g. Rajaratnam 1976), thereby confirming the appropriateness of the description.



### 6.2. Planar wake

The planar wake is an interesting case, since it features a nonzero ambient flow of amplitude  $U_\infty$ . This problem is statistically homogeneous in  $y$  and  $t$ . Applying the symmetries to (4.5), using that  $\bar{u}_x = (1 - \bar{\chi}_0)U_\infty$  at the interface and setting  $\zeta = z$ , we obtain

$$\bar{V}_n = \bar{u}_z - U_\infty \frac{dh_t}{dx}. \quad (6.4)$$

Using that  $dA = L_z dz$  and  $\bar{\mathcal{L}} = 2L_z$  (since the interface is present on both sides of the  $z = 0$  plane), (4.6) and (4.7) are given by

$$\frac{d}{dx} \int_{-h_t}^{h_t} \bar{u}_x dz = -2\bar{V}_n = 2 \left( U_\infty \frac{dh_t}{dx} - \bar{u}_z \right), \quad (6.5)$$

$$\frac{d}{dx} \int_{-h_t}^{h_t} \bar{u}_x^2 dz = 2U_\infty \left( U_\infty \frac{dh_t}{dx} - \bar{u}_z \right). \quad (6.6)$$

By substituting (6.5) into (6.6), assuming that  $\overline{u'_x u'_x} \ll \bar{u}_x^2$  and rearranging it follows that the mean momentum deficit  $\int_{-h_t}^{h_t} \bar{u}_x (U_\infty - \bar{u}_x) dz$  is conserved as expected (e.g. Pope 2000).

### 6.3. Temporal jet

The capability to directly quantify the entrainment velocity  $\bar{V}_n$  in temporal free shear flows (e.g. atmospheric boundary layers) is one of the useful results of the integral description put forward here. The distinguishing aspect of these flows is that they tend to be homogeneous in  $x$  and  $y$ . For example, for a temporal jet (Da Silva & Pereira 2008; van Reeuwijk & Holzner 2014), we can apply the symmetries to (4.5), and obtain

$$\bar{V}_n = -\frac{dh_t}{dt}. \quad (6.7)$$

Using that  $dA = L_z dz$  and  $\bar{\mathcal{L}} = 2L_z$ , (4.6) and (4.7) simplify to

$$2L_z \frac{dh_t}{dt} = -2L_z \bar{V}_n = 2L_z \frac{dh_t}{dt}, \quad (6.8)$$

$$L_z \frac{d}{dt} \int_{-h_t}^{h_t} \bar{u}_x dA = 0. \quad (6.9)$$

The first equation simply confirms that  $\bar{V}_n$  has been defined appropriately, whilst the second equation demonstrates the conservation of volume flux for this flow (van Reeuwijk & Holzner 2014).

The equivalence between the integrals of local and global entrainment, i.e. (5.2), was studied in van Reeuwijk & Holzner (2014). It was shown that for the temporal jet, the integral entrainment at the global and local entrainment are indeed identical over several decades of variation in  $\chi_0$  (enstrophy in this case), provided it was small enough. However, for the relatively low Reynolds number under consideration it was shown to be important to take into account the change in the interface location upon changing the threshold value  $\chi_0$  if one were to determine the entrainment coefficient  $\alpha$  from the local entrainment velocity. The consistency between the integral global and local entrainment flux (5.2) was shown also for the case of penetrative convection (Holzner & van Reeuwijk 2017) and an inclined temporal gravity current (van Reeuwijk *et al.* 2018).

## 6.4. Unsteady axisymmetric jets and plumes

Ensemble-averaged equations describing axisymmetric unsteady jets and plumes retain a dependence on three independent variables over which the flow is in homogeneous: the streamwise direction  $x$ , the lateral or normal direction  $r$ , and time  $t$ . In the case of unsteady jets and plumes, it cannot be assumed that the flow remains slender, since there is substantial variation of all the quantities of interest over short distances. Thus, we substitute the definitions of  $h_t$  and  $Q = 2 \int_0^{h_t} \bar{u}_x r dr$  into (4.3), which gives

$$\frac{\partial h_t^2}{\partial t} + \frac{\partial Q}{\partial x} = -\frac{1}{\pi} \oint_{\partial\bar{\Omega}} \frac{\bar{V}_n}{|\mathbf{N}_\perp|} d\ell, \quad (6.10)$$

where the right-hand side accords with our intuitive understanding of entrainment across a physically defined interface. Similarly, defining a specific momentum flux  $M = 2 \int_0^{h_t} \bar{u}_x^2 r dr$ , the *integral* or *top-hat* width  $h = Q/\sqrt{M}$  of an unsteady jet or plume obeys (Craske & van Reeuwijk 2016)

$$\frac{1}{\gamma} \frac{\partial h^2}{\partial t} + \frac{\partial Q}{\partial x} = 2\alpha M^{1/2}, \quad (6.11)$$

where  $\alpha$  is an entrainment coefficient that depends on dimensionless properties of the flow, such as the Richardson number, dimensionless streamwise gradients and parameters characterising the flow's radial dependence. The dimensionless parameter  $\gamma$  characterises the shape of the mean velocity in the plume as an integral of the mean flux of streamwise kinetic energy divided by  $M^2/Q$ . If one assumes self-similarity by introducing a similarity variable  $\eta = r/h$ , it directly follows that 1)  $h_t = \eta_t h$  where  $\eta_t$  is a constant; and 2) that  $\gamma$  is a constant (4/3 for a Gaussian profile). In this case, the terms in (6.10) and (6.11) can be matched individually with result

$$\eta_t = \gamma^{-1/2}, \quad \alpha = -\frac{1}{2\pi M^{1/2}} \oint_{\partial\bar{\Omega}} \frac{\bar{V}_n}{|\mathbf{N}_\perp|} d\ell \equiv \alpha_0. \quad (6.12)$$

Equation (6.12) shows that for an unsteady flow which remains self-similar, the global entrainment coefficient  $\alpha$  represents physical entrainment across its boundary  $h_t$ , entirely consistent with its classical interpretation.

However, in the vicinity of abrupt changes in the streamwise direction, unsteady jets and plumes depart significantly from self-similarity (Craske & van Reeuwijk 2015, 2016). In this case, the equivalence between the individual terms in (6.10) and (6.11) is lost. Consequently, the strongest statement that can be made regarding the entrainment coefficient is that

$$\alpha = \underbrace{-\frac{1}{2\pi M^{1/2}} \oint_{\partial\bar{\Omega}} \frac{\bar{V}_n}{|\mathbf{N}_\perp|} d\ell}_{\alpha_0} + \underbrace{\frac{1}{2M^{1/2}} \left( \frac{\partial}{\partial t} \left( \frac{h^2}{\gamma} - h_t^2 \right) + \frac{h^2}{\gamma^2} \frac{\partial \gamma}{\partial t} \right)}_{\alpha_1}. \quad (6.13)$$

The entrainment coefficient  $\alpha_0$  continues to account for fluid entrained across the TNTI and therefore has a direct physical interpretation. In contrast, the pseudo entrainment described by  $\alpha_1$  reconciles the definition of  $\alpha$ , as stated in (6.11) terms of  $Q$  and  $M$ , with entrainment across the TNTI during departures from self-similarity. It accounts for differences between temporal changes in the widths  $h$  and  $h_t$ , in addition to temporal changes in the parameter  $\gamma$ , which accounts for a change in the shape of the mean velocity profile.

If, in view of such difficulties, one is tempted to suggest that we should abandon (6.11) and focus on (6.10) instead, it should be noted that (6.11), unlike (6.10), can be

readily augmented with a conservation equation for momentum containing  $\partial_t Q + \partial_x M$  to produce a tractable model (Craske & van Reeuwijk 2016). Indeed, it is for this reason that establishing the connection between the local and global perspectives of entrainment is crucial.

## 7. Conclusions

Turbulent entrainment lies at the core of many important applications in engineering and science. This paper developed an integral description of turbulent free shear flows that develop in space and/or time. It connects local and global descriptions of turbulent entrainment, and provides a simple and clear notation to describe the intricacies of TNTI dynamics. The description relies on the relative velocity between the fluid and the scalar interface  $V_n$ . By applying this description, in which the interface is defined implicitly via the isosurface  $\chi = \chi_0$ , in a local manner, integral equations are obtained that explicitly feature the role local entrainment. Local entrainment is characterised by a large surface area and velocities of the order of the Kolmogorov scale (Corrsin & Kistler 1955). By using an average scalar field  $\chi_0$ , an equation for the global entrainment velocity  $\bar{V}_n$  was obtained, which resulted in equation (4.2) formulated in terms of the interface thickness  $h_t$ . The associated integral equations make a statement about global entrainment, which is characterised by surface areas and entrainment velocities of the order of the integral scales of the problem under consideration.

The special cases discussed in §6 apply the description to four canonical free shear flows, and help interpretation of the relation between global and local entrainment and of the entrainment coefficient. The description can easily be applied to other canonical free shear flows (e.g. plumes, unsteady free shear flows, cloudy boundary layers, gravity currents), and allows for further analysis, in particular using the recently developed entrainment decompositions techniques for local (Holzner & Luethi 2011) and global (van Reeuwijk & Craske 2015) descriptions of turbulent entrainment, and by linking entrainment to non-equilibrium turbulence (Zhou & Vassilicos 2017).

## Acknowledgements

M.v.R. and J.C.V. acknowledge financial support from the H2020 Innovative Training Network COMPLETE (grant agreement no 675675). M.v.R. was additionally supported by the EPSRC project Multi-scale Dynamics at the Turbulent/Non-turbulent Interface of Jets and Plumes (grant number EP/R043175/1). J.C. gratefully acknowledges an Imperial College Junior Research Fellowship award.

## Appendix A. Integral identities

In this appendix we derive the integral identities (2.3)-(2.5) by considering volume and time integrals over infinitesimal slices of size  $\delta x \rightarrow 0$  and  $\delta t \rightarrow 0$ , respectively. The identity (2.3) for the integral gradient operator can be obtained directly from (2.4) by substituting  $\mathbf{F} = \phi \mathbf{e}_i$  for  $i \in \{x, y, z\}$ ; we therefore only need to prove (2.4) and (2.5). We start with the proof of (2.4) which is a generalisation of the method introduced by Zhou & Vassilicos (2017) in their Appendix. The first step is to decompose  $\int_{\Omega} \nabla \cdot \mathbf{F} dA$  as follows:

$$\int_{\Omega} \nabla \cdot \mathbf{F} dA = \int_{\Omega} \frac{\partial F_x}{\partial x} dA + \int_{\Omega} \nabla \cdot_{\perp} \mathbf{F}_{\perp} dA = \int_{\Omega} \frac{\partial F_x}{\partial x} dA - \oint_{\partial\Omega} \mathbf{F}_{\perp} \cdot \mathbf{n} dl, \quad (\text{A } 1)$$

where use is made of Gauss's divergence theorem (cf. Stokes' theorem in appendix B) in the  $y - z$  plane and  $\mathbf{n} = \mathbf{N}_\perp/|\mathbf{N}_\perp| = \nabla_\perp\chi/|\nabla_\perp\chi|$  is the surface normal in the  $y - z$  plane. Note that the minus sign in the last term of (A 1) originates from the fact that  $\mathbf{n}$  points *into*  $\Omega$  rather than outwards.

We now seek a formula for commuting  $\int_\Omega$  and  $\partial/\partial x$  in (A 1). Note that

$$\begin{aligned} \frac{\partial}{\partial x} \int_\Omega F_x dA &= \lim_{\delta x \rightarrow 0} \frac{1}{\delta x} \left( \int_{\Omega(x+\delta x)} F_x(x+\delta x) dA - \int_{\Omega(x)} F_x(x) dA \right) \\ &= \int_{\Omega(x)} \frac{\partial F_x}{\partial x} dA + \lim_{\delta x \rightarrow 0} \frac{1}{\delta x} \left[ \int_{\Omega(x+\delta x)} F_x(x+\delta x) dA - \int_{\Omega(x)} F_x(x+\delta x) dA \right]. \end{aligned} \quad (\text{A } 2)$$

The bracketed term in (A 2) is the difference between the surface integrals of  $F_x(x+\delta x)$  over  $\Omega(x+\delta x)$  and over  $\Omega(x)$  respectively. This integral is crucially related to the slope of the interface with the  $x$ -direction,  $N_x/|\mathbf{N}_\perp|$ . Indeed, the amount of substance flowing into  $\Omega$  at a certain location on the interface due to the slope is equal to  $F_x \delta h_t \delta \ell$ , where  $\delta h_t$  is the change in the interface position in the  $y - z$  plane (normal to  $\delta \ell$ ) over the streamwise distance  $\delta x$ . Since  $\delta h_t = N_x/|\mathbf{N}_\perp| \delta x$  (Figure 1b), it follows that the difference between the two surface integrals is, to leading order, equal to the curvilinear integral  $\oint_{\partial\Omega} F_x(x+\delta x) N_x/|\mathbf{N}_\perp| \delta x d\ell$ . Hence, (A 2) becomes

$$\frac{\partial}{\partial x} \int_\Omega F_x dA = \int_\Omega \frac{\partial F_x}{\partial x} dA + \oint_{\partial\Omega} F_x \frac{N_x}{|\mathbf{N}_\perp|} d\ell. \quad (\text{A } 3)$$

Combining (A 3) with (A 1) leaves us with our first main general result, identity (2.4).

In the case where  $\mathbf{F} = Q\mathbf{u}$  for some field  $Q$ , we have  $F_x(x)N_x/|\mathbf{N}_\perp| = Q(x)u_x(x)N_x/|\mathbf{N}_\perp|$ . Defining  $dt$  to be the time required for a fluid element to move a distance  $dx = u_x dt$  in the streamwise direction, Zhou & Vassilicos (2017) defined the pseudo-velocity  $dh_t/dt$  which they termed  $V_n$  (not to be confused with the definition of  $V_n$  in the present paper). Given that their  $V_n$  equals  $u_x(x)N_x/|\mathbf{N}_\perp|$ ,  $\oint_{\partial\Omega} F_x(x)N_x/|\mathbf{N}_\perp| d\ell = \oint_{\partial\Omega} Q(x)V_n N_x/|\mathbf{N}_\perp| d\ell$  in terms of their pseudo-velocity  $V_n$  (see also section B.2 of Appendix B). This establishes the correspondence between the results in their Appendix (which they gave for  $Q = 1$ ) and (A 3), (2.4) here.

We now proceed with the proof of identity (2.5). Integrating the material derivative over  $\Omega$  yields

$$\int_\Omega \frac{D\phi}{Dt} dA = \int_\Omega \frac{\partial \phi}{\partial t} dA + \int_\Omega \nabla \cdot (\phi \mathbf{u}) dA - \int_\Omega \phi \nabla \cdot \mathbf{u} dA \quad (\text{A } 4)$$

and then making use of (2.4) for  $\mathbf{F} = \phi \mathbf{u}$ ,

$$\int_\Omega \frac{D\phi}{Dt} dA = \int_\Omega \frac{\partial \phi}{\partial t} dA + \frac{\partial}{\partial x} \int_\Omega \phi u_x dA - \oint_{\partial\Omega} \phi \mathbf{u} \cdot \frac{\mathbf{N}}{|\mathbf{N}_\perp|} d\ell - \int_\Omega \phi \nabla \cdot \mathbf{u} dA. \quad (\text{A } 5)$$

Following (A 2), we now wish to commute  $\int_\Omega$  and  $\partial/\partial t$ :

$$\begin{aligned} \frac{\partial}{\partial t} \int_\Omega \phi dA &= \lim_{\delta t \rightarrow 0} \frac{1}{\delta t} \left( \int_{\Omega(t+\delta t)} \phi(t+\delta t) dA - \int_{\Omega(t)} \phi(t) dA \right) \\ &= \int_{\Omega(t)} \frac{\partial \phi}{\partial t} dA + \lim_{\delta t \rightarrow 0} \frac{1}{\delta t} \left[ \int_{\Omega(t+\delta t)} \phi(t+\delta t) dA - \int_{\Omega(t)} \phi(t+\delta t) dA \right]. \end{aligned} \quad (\text{A } 6)$$

The bracketed term in (A 6) is the difference between the surface integrals of  $\phi(t+\delta t)$  over  $\Omega(t+\delta t)$  and over  $\Omega(t)$  respectively. The interface, which moves at normal velocity

$v_n = \mathbf{v} \cdot \mathbf{N}$ , will move at velocity  $v_n/|\mathbf{N}_\perp|$  when projected onto the  $y - z$  plane. Thus, over a time increment  $\delta t$ , the interface element of length  $\delta \ell$  will sweep an area in the  $y - z$  plane equal to  $-v_n/|\mathbf{N}_\perp| \delta t \delta \ell$  (the minus sign once more originates from the inward pointing normal  $\mathbf{N}$ ). This implies that difference between the two surface integrals in (A 6) is, to leading order, equal to the curvilinear integral  $-\oint_{\partial\Omega} \phi(t + \delta t) v_n/|\mathbf{N}_\perp| \delta t d\ell$ . Hence, (A 6) becomes

$$\frac{\partial}{\partial t} \int_{\Omega} \phi dA = \int_{\Omega} \frac{\partial \phi}{\partial t} dA - \oint_{\partial\Omega} \phi \frac{v_n}{|\mathbf{N}_\perp|} d\ell. \quad (\text{A } 7)$$

Combining (A 7) with (A 5) and invoking the relative iso-surface velocity  $\mathbf{V} = \mathbf{v} - \mathbf{u}$ , leaves us with our second main general result, identity (2.5), i.e.

$$\int_{\Omega} \frac{D\phi}{Dt} dA = \frac{\partial}{\partial t} \int_{\Omega} \phi dA + \frac{\partial}{\partial x} \int_{\Omega} u_x \phi dA + \oint_{\partial\Omega} \frac{V_n}{|\mathbf{N}_\perp|} \phi d\ell - \int_{\Omega} \phi \nabla \cdot \mathbf{u} dA.$$

Noting that the approaches used in (A 2) and (A 6) are equivalent and account for the commutation of integration with differentiation with respect to either time or space, we abstract and generalise our results using differential geometry in the following section.

## Appendix B. Differential geometry

In this appendix we regard the region  $\Omega$ , defined by an isosurface of  $\chi$ , as a submanifold whose shape changes as a function of *codimensions*  $x$  and  $t$ , for example. In manipulating integrals of partial derivatives over  $\Omega$ , one is faced with two distinct types of expression. The first involves derivatives in directions that lie within the dimensions of  $\Omega$  and the second involves derivatives in directions that lie in the codimension of  $\Omega$ . The first can be manipulated using a generalised version of Stokes' theorem, whilst the second require a generalised form of Leibniz's rule for commuting integration and partial differentiation. The first involve physical fluxes and velocities at the boundary  $\partial\Omega$ . The second, in contrast, involve pseudo fluxes and velocities that account for deformations of the integration domain with respect to changes in a given codimension. Since the integration domain is specified by  $\chi$  independently of physical boundary fluxes, the two are independent.

To crystallise these ideas, consider an  $n$ -dimensional slice  $\Omega$  through an  $N$ -dimensional manifold defined by  $\chi(\mathbf{x}, \mathbf{y}) \geq \chi_0$  by fixing  $m = N - n$  codimensions  $\mathbf{x}$ , as depicted in figure 3. The slice itself can be traversed locally by coordinates  $y^1, \dots, y^n$ . Components of a differential  $N - 1$  form  $\omega$  can be partitioned into fluxes  $f$  and  $g$  that are either normal to tangential to the area form  $dA = dy^1 \wedge dy^2 \wedge \dots \wedge dy^n$ , respectively. For example, if  $x^1 = x$ ,  $y^1 = y$  and  $y^2 = z$ , a flux  $\omega$  can be partitioned:

$$\omega = \underbrace{\omega_x dy \wedge dz}_f + \underbrace{\omega_y dz \wedge dx + \omega_z dx \wedge dy}_g. \quad (\text{B } 1)$$

Integrals of the  $N$ -form  $dg$  at a given point in the codomain can be evaluated using a generalised version of the fundamental theorem of calculus in the form of Stokes' theorem. With slight abuse of notation, because  $dg$  is an  $N$ -form rather than an  $n$ -form, we express the application of Stokes' theorem over the slice  $\Omega$  as

$$\int_{\Omega} dg = \int_{\partial\Omega} g, \quad (\text{B } 2)$$

which we will refer to as a *partial integral* (Whitney 2005) that results in a differential

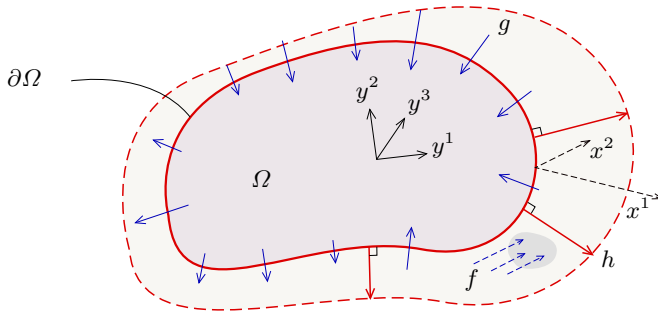


FIGURE 3. A submanifold  $\Omega$  described by local coordinates  $y^1, \dots, y^n$  and parameterised over codimensions  $x^1, \dots, x^m$ . The physical flux in the plane of  $\Omega$  corresponds to the  $(m+n-1)$ -form  $g$  and the pseudo flux arising from the normal flux  $f$  through deformations in  $\partial\Omega$  as one moves with unit ‘velocity’ in the direction  $x^i$  corresponds to the  $(m+n-1)$ -form  $h$ .

form containing, in the case of (B2),  $dx^1 \wedge \dots \wedge dx^m$ . A more rigorous treatment of the operation would consider integrals along a *fibre* ( $\Omega$ ) of a *fibre bundle* (the entire space). In either case, equation (B2) states that integrals of derivatives with respect to  $y^1 \dots, y^n$  can be evaluated as surface integrals that account for boundary transport.

The manipulation  $df$  is fundamentally different from  $dg$  because  $df$ , unlike  $dg$ , involves partial derivatives with respect to the codimensions  $x^1, \dots, x^m$ . Consequently, partial integrals of  $df$  over  $\Omega$  satisfy a generalised version of Leibniz’s rule that specifies how to commute integration with exterior differentiation:

$$\int_{\Omega} df = d \int_{\Omega} f - \int_{\partial\Omega} h, \quad (\text{B3})$$

in which the partial integral of  $f$  over  $\Omega$  produces an  $(m-1)$ -form to which the exterior derivative  $d$  can be applied. The final term in (B3) contains  $h$ , which is a differential  $(N-1)$ -form corresponding to a *pseudo* flux, in contrast with the physical flux  $g$ . The *pseudo* flux  $h$  results from  $f$  and the dependence of  $\Omega$  on the codimensions, and therefore depends on the geometry of the surface  $\chi - \chi_0$ .

To determine  $h$ , we define a vector  $Y$  that is tangent to  $\Omega$ , is perpendicular to an isosurface of  $\chi$ :

$$(\nabla_{\chi} \lrcorner dA)(Y) = \mathbf{0}, \quad (\text{B4})$$

and corresponds to a unit rate of change down  $\chi$ , such that  $d\chi(Y) = -1$ . Consequently, the vector  $(\partial_{x^i} \chi)Y$  acts in a direction that is perpendicular to  $\partial\Omega$  and describes the change in  $\partial\Omega$  that occurs as one moves with unit ‘velocity’ along the  $i^{\text{th}}$  codimension. The effect of changes in  $\Omega$  on integrals is captured by Cartan’s magic formula for the Lie derivative  $X \lrcorner d\omega = \mathcal{L}_X \omega - d(X \lrcorner \omega)$ , where  $\mathcal{L}_X \omega$  describes the change in  $\omega$  along the flow defined by  $X$ . Setting  $X = \partial_{x^i} + (\partial_{x^i} \chi)Y$  and focusing on each component  $f_i$  of  $f$  in (B1), leads to a generalised version of Leibniz’s rule (see, for example, Flanders 1973) for partial integration over  $\Omega$ :

$$\int_{\Omega} \frac{\partial}{\partial x^i} \lrcorner df_i = \frac{\partial}{\partial x^i} \int_{\Omega} f_i - \int_{\partial\Omega} \frac{\partial \chi}{\partial x^i} Y \lrcorner f_i, \quad (\text{B5})$$

is an  $(m-1)$ -form. Applying  $dx^i \wedge$  to (B5), and summing over each codimension  $i$ , shows that each term in (B5) corresponds to the respective terms in (B3) and therefore reveals

that

$$h = Y \lrcorner (d\chi \wedge f), \quad (\text{B6})$$

which is fundamental in determining the boundary contribution of fluxes that are perpendicular to  $dA$ . Combining (B6) with (B2) and (B3) leads to a general formula for commuting exterior differentiation and partial integration over a submanifold:

$$\int_{\Omega} d\omega - d \int_{\Omega} \omega = \underbrace{\int_{\partial\Omega} g}_{\text{Stokes}} - \underbrace{\int_{\partial\Omega} h}_{\text{Leibniz}}. \quad (\text{B7})$$

As illustrated in figure 3, the commutation of integration and exterior differentiation leads to physical fluxes  $g$  in the plane of  $dA$  in addition to *pseudo* fluxes  $h$ , which account for the flow  $f$  through the contraction and expansion of  $\Omega$  as the codimensions  $t$  and  $x$  change.

### B.1. Example: integration of $D\phi/Dt$ over $\Omega(x, t) \ni (y, z)$

To integrate  $D\phi/Dt$  over an area  $\Omega(x, t)$ , we identify  $x^1 = t$ ,  $x^2 = x$  as the submanifold's codimensions and  $y^1 = y$ ,  $y^2 = z$  as the submanifold's coordinates. We decompose  $D\phi/Dt$  to incorporate the divergence of a flux  $\omega$  and indicate the correspondance with  $d\omega = df + dg$ :

$$\frac{D\phi}{Dt} = \underbrace{\frac{\partial\phi}{\partial t} + \frac{\partial u_x\phi}{\partial x}}_{df} + \underbrace{\frac{\partial u_y\phi}{\partial y} + \frac{\partial u_z\phi}{\partial z}}_{dg} - \phi \nabla \cdot \mathbf{u}, \quad (\text{B8})$$

which, regarding  $D\phi/Dt$  as a differential 4-form, implies that

$$\omega = \underbrace{\phi dx \wedge dy \wedge dz - u_x \phi dt \wedge dy \wedge dz}_{f} + \underbrace{u_y \phi dt \wedge dx \wedge dz - u_z \phi dt \wedge dx \wedge dy}_{g}. \quad (\text{B9})$$

Here, the tangent vector  $Y$  is:

$$Y = Y_y \frac{\partial}{\partial y} + Y_z \frac{\partial}{\partial z} = - \left( \left( \frac{\partial\chi}{\partial y} \right)^2 + \left( \frac{\partial\chi}{\partial z} \right)^2 \right)^{-1} \left( \frac{\partial\chi}{\partial y} \frac{\partial}{\partial y} + \frac{\partial\chi}{\partial z} \frac{\partial}{\partial z} \right), \quad (\text{B10})$$

which, using (B7) and omitting the  $dt \wedge dx$  that remains after partial integration, results in

$$\begin{aligned} \int_{\Omega} \frac{D\phi}{Dt} dA &= \frac{\partial}{\partial t} \int_{\Omega} \phi dA + \frac{\partial}{\partial x} \int_{\Omega} u_x \phi dA + \int_{\partial\Omega} \left( Y_z \frac{\partial\chi}{\partial t} + u_x Y_z \frac{\partial\chi}{\partial x} + u_z \right) \phi dy \\ &\quad - \int_{\partial\Omega} \left( Y_y \frac{\partial\chi}{\partial t} + u_x Y_y \frac{\partial\chi}{\partial x} + u_y \right) \phi dz - \int_{\Omega} \phi \nabla \cdot \mathbf{u} dA. \end{aligned} \quad (\text{B11})$$

Identities for the integral of  $\nabla\phi$  and the area of  $\Omega$  can be obtained as corollaries of (B11) by substitution of  $\mathbf{u} = (1, 1, 1)^T$  and  $\phi = 1$ , respectively.

### B.2. Summary and connection with appendix A

Our results indicate that the commutation of integration and differentiation leads to storage terms and *pseudo* boundary fluxes that depend on the  $t$  and  $x$  dependence of the domain of integration. Such fluxes are distinct from the physical boundary fluxes that are obtained by applying Stokes' theorem to the divergence of fluxes that are tangential

to the domain of integration and arise from Leibniz's rule for differentiation under an integral sign.

To link (B 7) with appendix A it is necessary to note that the vector  $Y$  introduced at (B 4), and written explicitly in (B 10), corresponds to  $-\mathbf{n}/|\nabla_{\perp}\chi|$  and that

$$\frac{\partial\chi}{\partial t} = -v_n|\nabla\chi|, \quad \frac{\partial\chi}{\partial x} = u_x N_x|\nabla\chi|. \quad (\text{B } 12)$$

As made explicit in the fourth term of (B 11), each term in the integral of  $h$  accounts for  $Y$ , which is normal to  $\partial\Omega$  according to (B 4), scaled by either  $\partial_t\chi$  or  $\partial_x\chi$ . Consequently, by expanding (2.5) for  $\phi = 1$ , using (B 12) and recalling that  $|\mathbf{N}_{\perp}| = |\nabla_{\perp}\chi|/|\nabla\chi|$ ,

$$\frac{\partial}{\partial t} \int_{\Omega} dA + \frac{\partial}{\partial x} \int_{\Omega} u_x dA = \oint_{\partial\Omega} \underbrace{\mathbf{u} \cdot \mathbf{n} d\ell}_g - \oint_{\partial\Omega} \underbrace{\frac{v_n}{|\mathbf{N}_{\perp}|} - u_x \frac{N_x}{|\mathbf{N}_{\perp}|}}_h d\ell, \quad (\text{B } 13)$$

which is a special case of the relation (B 7). The inward boundary flux  $g = \mathbf{u} \cdot \mathbf{n} d\ell$  results from Stokes' theorem and is identical to  $V_f d\ell$  in Zhou & Vassilicos (2017). In contrast, the pseudo fluxes  $h$  result from Leibniz's rule for commuting integration and differentiation. The terms in  $h$  correspond to perpendicular fluxes through contractions and expansions of the boundary  $\partial\Omega$  as one traverses the *codimensions*  $t$  and  $x$  with unit velocity (see figure 3). Specifically, the term  $u_x N_x/|\mathbf{N}_{\perp}| d\ell$  corresponds to the increase in volume flux due to changes in the location of  $\partial\Omega$  as one moves, one unit in the  $x$  direction and is identical to  $V_n d\ell$  in Zhou & Vassilicos (2017) (stressing, again, that this  $V_n$  is not the same as the  $V_n$  defined in the present paper).

A practical advantage of the abstract approach adopted in appendix B is that the resulting surface integrals (see (B 11), for example) are given explicitly in terms of coordinate differentials  $dy$ ,  $dz$ . The integral expressions can therefore be readily evaluated on a numerical grid and, since differential forms  $dy$ ,  $dz$ ,  $dy \wedge dz$  have an orientation, automatically account for the orientation of a surface and its normal.

## REFERENCES

- BISSET, D. K., HUNT, J. C. R. & ROGERS, M. M. 2002 The turbulent/non-turbulent interface bounding a far wake. *J. Fluid Mech.* **451**, 383–410.
- BURRIDGE, H. C., PARKER, D. A., KRUGER, E. S., PARTRIDGE, J. L. & LINDEN, P. F. 2017 Conditional sampling of a high Péclet number turbulent plume and the implications for entrainment. *J. Fluid Mech.* **823**, 26–56.
- CANTWELL, B. & COLES, D. 1983 An experimental study of entrainment and transport in the turbulent near wake of a circular cylinder. *J. Fluid Mech.* **136**, 321–374.
- CORRSIN, S. & KISTLER, A.L 1955 Free stream boundaries of turbulent flows. *Tech. Rep.* 1244. NACA.
- CRASKE, J. & VAN REEUWIJK, M. 2015 Energy dispersion in turbulent jets. Part 1. Direct simulation of steady and unsteady jets. *J. Fluid Mech.* **763**, 500–537.
- CRASKE, J. & VAN REEUWIJK, M. 2016 Generalised unsteady plume theory. *J. Fluid Mech.* **792**, 1013–1052.
- DA SILVA, C. B., HUNT, J. C. R., EAMES, I. & WESTERWEEL, J. 2014 Interfacial layers between regions of different turbulence intensity. *Annu. Rev. Fluid Mech.* **46**, 567–590.
- DA SILVA, C. B. & MÉTAIS, O. 2002 On the influence of coherent structures upon interscale interactions in turbulent plane jets. *J. Fluid Mech.* **473**, 103–145.
- DA SILVA, C. B. & PEREIRA, J. C. F. 2008 Invariants of the velocity-gradient, rate-of-strain, and rate-of-rotation tensors across the turbulent/nonturbulent interface in jets. *Phys. Fluids* **20** (5), 055101.



- DE WIT, L., VAN RHEE, C. & KEETELS, G. 2014 Turbulent interaction of a buoyant jet with cross-flow. *J. Hydr. Eng.* **140** (12), 04014060.
- DEARDORFF, J. W., WILLIS G. E. STOCKTON B. H. 1980 Laboratory studies of the entrainment zone of a convectively mixed layer. *J. Fluid Mech.* **100**, 41–64.
- DEVENISH, B.J., ROONEY, G.G. & THOMSON, D.J. 2010 Large-eddy simulation of a buoyant plume in uniform and stably stratified environments. *J. Fluid Mech.* **652**, 75 – 103.
- FERNANDO, H. J. S. 1991 Turbulent mixing in stratified fluids. *Annu. Rev. Fluid Mech.* **23**, 455–493.
- FLANDERS, HARLEY 1973 Differentiation under the integral sign. *American Math. Monthly* **80** (6), 615–627.
- GARCIA, J.R. & MELLADO, J.P. 2014 The two-layer structure of the entrainment zone in the convective boundary layer. *J. Atmos. Sci.* **71**, 1935–1955.
- HEAD, M.R. 1958 Entrainment in the turbulent boundary layer. Reports & Memoranda 3152. Ministry of Aviation.
- HOLZNER, M. & LUETHI, B. 2011 Laminar superlayer at the turbulence boundary. *Phys. Rev. Lett.* **106** (13), 134503.
- HOLZNER, M. & VAN REEUWIJK, M. 2017 The turbulent/nonturbulent interface in penetrative convection. *J. Turbul.* **18**, 260–270.
- HUNT, G.R. & BURRIDGE, H.C. 2015 Fountains in industry and nature. *Annu. Rev. Fluid Mech.* **47**, 195–220.
- HUNT, J. C. R., ROTTMAN, J. W. & BRITTER, R. E. 1983 Some physical processes involved in the dispersion of dense gases. In *Proc. UITAM Symp. on Atmospheric Dispersion of Heavy Gases and Small Particles* (ed. G. Ooms & H. Tennekes), pp. 361–395. Springer.
- HUSSEIN, H. J., CAPP, S. P. & GEORGE, W. K. 1994 Velocity measurements in a high-Reynolds number, momentum-conserving, axisymmetric, turbulent jet. *J. Fluid Mech.* **258**, 31–75.
- JAHANBAKHSI, R. & MADNIA, C. 2018 The effect of heat release on the entrainment in a turbulent mixing layer. *J. Fluid Mech.* **844**.
- JONKER, H.J.J., VAN REEUWIJK, M., SULLIVAN, P. & PATTON, E. 2013 On the scaling of shear-driven entrainment: A DNS study. *J. Fluid Mech.* **732**, 150–165.
- KATO, H. & PHILLIPS, O. M. 1969 On the penetration of a turbulent layer into stratified fluid. *J. Fluid Mech.* **37**, 643–655.
- KOTSOVINOS, N. E. 1978 A note on the conservation of the volume flux in free turbulence. *J. Fluid Mech.* **86**, 201–203.
- KOTSOVINOS, N. E. & LIST, E. J. 1977 Plane turbulent buoyant jets. Part 1. Integral properties. *J. Fluid Mech.* **81** (01), 25–44.
- KRUG, D., CHUNG, D., PHILIP, J. & MARUSIC, I. 2017 Global and local aspects of entrainment in temporal plumes. *J. Fluid Mech.* **812**, 222–250.
- KRUG, D., HOLZNER, M., LUETHI, B., WOLF, M., KINZELBACH, W. & TSINOBER, A. 2015 The turbulent/non-turbulent interface in an inclined dense gravity current. *J. Fluid Mech.* **765**, 303–324.
- LIST, E. J. 1982 Turbulent jets and plumes. *Annu. Rev. Fluid Mech.* **14** (1), 189–212.
- MAHESH, K. 2013 The interaction of jets with cross-flow. *Annu. Rev. Fluid Mech.* **45**, 379–407.
- MELLADO, JP. 2012 Direct numerical simulation of free convection over a heated plate. *J. Fluid Mech.* **712**, 418–450.
- MELLADO, J. P. 2017 Cloud-top entrainment in stratocumulus clouds. *Annu. Rev. Fluid Mech.* **49** (1), 145–169.
- OBLIGADO, M., DAIRAY, T. & VASSILICOS, J. C. 2016 Nonequilibrium scalings of turbulent wakes. *Phys. Rev. Fluids* **1** (4), 044409.
- ODIER, P., CHEN, J. & ECKE, R. E. 2014 Entrainment and mixing in a laboratory model of oceanic overflow. *J. Fluid Mech.* **746**, 498–535.
- PHILIP, J., MENEVEAU, C., DE SILVA, C. M. & MARUSIC, I. 2014 Multiscale analysis of fluxes at the turbulent/non-turbulent interface in high Reynolds number boundary layers. *Phys. Fluids* **26**, 015105.
- POPE, S. B. 2000 *Turbulent flows*. Cambridge University Press.
- RAJARATNAM, N. 1976 *Turbulent Jets. Developments in Water Science* 5. Elsevier.
- REDFORD, J. A., CASTRO, I. P. & COLEMAN, G. N. 2012 On the universality of turbulent axisymmetric wakes. *J. Fluid Mech.* **710**, 419–452.

- VAN REEUWIJK, M. & CRASKE, J. 2015 Energy-consistent entrainment relations for jets and plumes. *J. Fluid Mech.* **782**, 333 – 355.
- VAN REEUWIJK, M. & HOLZNER, M. 2014 The turbulence boundary of a temporal jet. *J. Fluid Mech.* **739**, 254–275.
- VAN REEUWIJK, M., HOLZNER, M. & CAULFIELD, C. P. 2019 Mixing and entrainment are suppressed in inclined gravity currents. *J. Fluid Mech.* **873**, 786–815.
- VAN REEUWIJK, M., KRUG, D. & HOLZNER, M. 2018 Small-scale entrainment in inclined gravity currents. *Environ. Fluid Mech.* **18** (1), 225–239.
- DE ROOY, W.C. *et al.* 2013 Entrainment and detrainment in cumulus convection: an overview. *Quart. J. Roy. Meteor. Soc.* **139** (670), 1–19.
- SCASE, M. M., CAULFIELD, C. P., DALZIEL, S. B. & HUNT, J. C. R. 2006 Time-dependent plumes and jets with decreasing source strengths. *J. Fluid Mech.* **563**, 443–461.
- SILLERO, J.A., JIMENEZ, J. & MOSER, R.D. 2013 One-point statistics for turbulent wall-bounded flows at Reynolds numbers up to  $\delta^+ \approx 2000$ . *Phys. Fluids* **25**, 105102.
- SILVA, T. S., ZECCHETTO, M. & DA SILVA, C. B. 2018 The scaling of the turbulent/non-turbulent interface at high Reynolds numbers. *J. Fluid Mech.* **843**, 156–179.
- SREENIVASAN, K. R., RAMSHANKAR, R. & MENEVEAU, C. 1989 Mixing, entrainment and fractal dimensions of surfaces in turbulent flows. *Proc. Roy. Soc. A -Math. Phys. Eng. Sci.* **421** (1860), 79.
- SULLIVAN, P. P., MOENG, C. H., STEVENS, B., LENSCHOW, D. H. & MAYOR, S. D. 1998 Structure of the entrainment zone capping the convective atmospheric boundary layer. *J. Atmos. Sci.* **55**, 3042–3064.
- TURNER, J. S. 1962 The ‘starting plume’ in neutral surroundings. *J. Fluid Mech.* **13** (03), 356–368.
- TURNER, J. S. 1986 Turbulent entrainment: the development of the entrainment assumption, and its application to geophysical flows. *J. Fluid Mech.* **173**, 431–471.
- WATANABE, T., RILEY J. DE BRUYN KOPS S. DIAMESSIS P. & ZHOU Q. 2016 Turbulent/non-turbulent interfaces in wakes in stably stratified fluids. *J. Fluid Mech.* **797**, R1.
- WATANABE, T., RILEY, J., NAGATA, K., ONISHI, R. & MATSUDA, K. 2018 A localized turbulent mixing layer in a uniformly stratified environment. *J. Fluid Mech.* **849**, 245–276.
- WATANABE, T., SAKAI, Y., NAGATA, K., ITO, Y. & HAYASE, T. 2014 Enstrophy and passive scalar transport near the turbulent/non-turbulent interface in a turbulent planar jet flow. *Phys. Fluids* **26** (10), 105103.
- WELLS, M., CENEDESE, C. & CAULFIELD, C. P. 2010 The relationship between flux coefficient and entrainment ratio in density currents. *J. Phys. Oceanogr.* **40** (12), 2713–2727.
- WESTERWEEL, J., FUKUSHIMA, C., PEDERSEN, J. M. & HUNT, J. C. R. 2005 Mechanics of the turbulent-nonturbulent interface of a jet. *Phys. Rev. Lett.* **95** (17), 174501.
- WHITNEY, H. 2005 *Geometric Integration Theory*. Dover.
- WOODHOUSE, M. J., PHILLIPS, J. C. & HOGG, A. J. 2016 Unsteady turbulent buoyant plumes. *J. Fluid Mech.* **794**, 595–638.
- WOODS, A. W. 2010 Turbulent plumes in nature. *Annu. Rev. Fluid Mech.* **42**, 391–412.
- XU, YUNXIU, FERNANDO, HARINDRA J. S. & BOYER, DON L. 1995 Turbulent wakes of stratified flow past a cylinder. *Physics of Fluids* **7** (9), 2243–2255.
- ZHOU, Y. & VASSILICOS, J.C. 2017 Related self-similar statistics of the turbulent/non-turbulent interface and the turbulence dissipation. *J. Fluid Mech.* **821**, 440–457.